

Vacuum Ultraviolet Absorption Array Spectrometer As a Selective Detector for Comprehensive Two-Dimensional Gas Chromatography: Concept and First Results

Thomas Gröger,^{*,†,‡,⊥} Beate Gruber,^{†,‡,⊥} Dale Harrison,[§] Mohammad Saraji-Bozorgzad,^{||} Makhosazana Mthembu,[‡] Aimée Sutherland,^{†,‡} and Ralf Zimmermann^{†,‡}

[†]Joint Mass Spectrometry Centre, Comprehensive Molecular Analytics, Helmholtz Zentrum München, Ingolstädter Landstrasse 1, 85764 Neuherberg, Germany

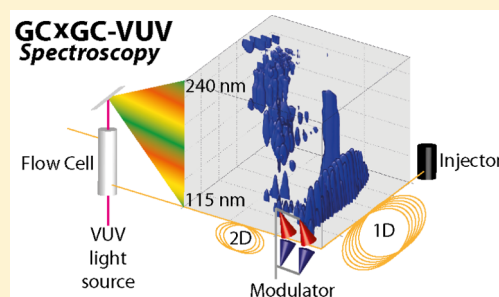
[‡]Joint Mass Spectrometry Centre, Chair of Analytical Chemistry, University of Rostock, Dr. Lorenz Weg 1, 85764 Rostock, Germany

[§]VUV Analytics, Inc., Austin, Texas 78717, United States

^{||}Photonion GmbH, Hagenower Strasse 73, 19061 Schwerin, Germany

Supporting Information

ABSTRACT: Fast and selective detectors are very interesting for comprehensive two-dimensional gas chromatography (GC × GC). This is particularly true if the detector system can provide additional spectroscopic information on the compound structure and/or functionality. Other than mass spectrometry (MS), only optical spectroscopic detectors are able to provide selective spectral information. However, until present the application of optical spectroscopy technologies as universal detectors for GC × GC has been restricted mainly due to physical limitations such as insufficient acquisition speed or high detection limits. A recently developed simultaneous-detection spectrometer working in the vacuum ultraviolet (VUV) region of 125–240 nm overcomes these limitations and meets all the criteria of a universal detector for GC × GC. Peak shape and chromatographic resolution is preserved and unique spectral information, complementary to mass spectrometry data, is gained. The power of this detector is quickly recognized as it has the ability to discriminate between isomeric compounds or difficult to separate structurally related isobaric species; thus, it provides additional selectivity. A further promising feature of this detector is the data analysis concept of spectral filtering, which is accomplished by targeting special electronic transitions that allows for a fast screening of GC × GC chromatograms for designated compound classes.



Comprehensive two-dimensional gas chromatography (GC × GC) is a powerful instrumental analytical technology for the separation of compounds from highly complex samples containing hundreds or thousands of vaporizable compounds.¹ The first applied detection systems for GC × GC was the nonselective flame ionization detector (FID) for the detection of organic compounds.^{2–4} Although an FID is an excellent detector for quantitative studies, qualitative analysis of highly complex samples by means of retention time matching is challenging. However, other more selective but nonspectroscopic GC detection methods such as thermionic detection, electron capture, or chemiluminescence may suffer either in sensitivity and/or acquisition speed; nonetheless, they have been successfully applied in combination with GC × GC.⁴ It is known that for some applications the high chromatographic separation power of GC × GC reduces the need for selective detection systems, but the analysis of extremely complex samples such as petrochemical fractions,^{5–7} ambient aerosols,^{8–10} forensic,^{11–13} or metabolic samples^{14–17} remains challenging, even with the high separation power of GC × GC. This is in particular true regarding the identification of

unknown compounds in nontargeted analytical approaches if the differentiation of isomeric compounds or compounds with similar separation and mass spectrometric properties (e.g., cycloalkanes and alkenes) has to be addressed. For this reason almost all of the commonly used detectors for one-dimensional gas chromatography (GC) have been adapted and tested for their applicability as a GC × GC detector to gather as much selective information as possible about the separated compounds. However, there are important requirements for GC × GC detectors; these detectors need to have a large dynamic range, a high acquisition frequency, as well as exhibit sensitivity and selectivity.¹⁸ Currently, the only detectors which meet all of the above-mentioned criteria in a sufficient manner, are fast mass spectrometric detection systems like time-of-flight mass spectrometer (TOFMS) or the latest generation quadrupole mass spectrometer (QMS).²⁰ Even though these MS

Received: July 2, 2015

Accepted: January 25, 2016

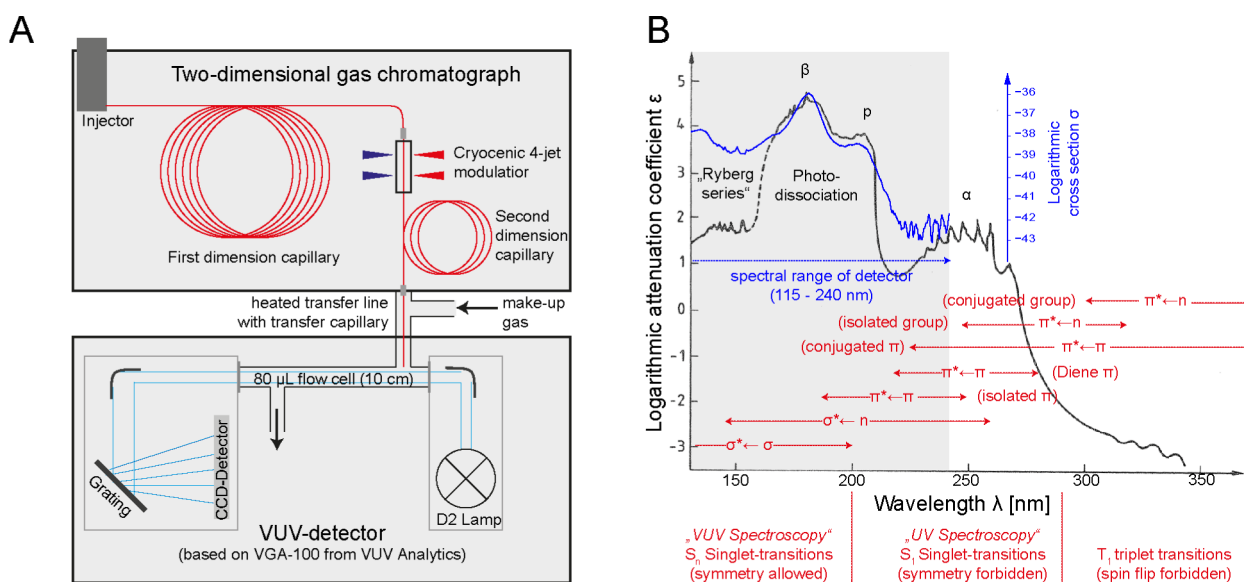


Figure 1. (A) Instrumental setup of the comprehensive two-dimensional gas chromatography-VUV-absorption spectrometer (GC × GC-VUV). (B) VUV-absorption spectrum of benzene (gas phase) with assignment of electronic transitions. Blue, spectra acquired with VUV-spectrometer; black, reference from the literature¹⁹ (with kind permission of Springer, Copyright 1985). In the VUV-region (~170 nm) the absorption cross section is between two and 3 orders of magnitude larger than in the classical UV absorption range (up to 250 nm).

66 detectors **has** been already established as standard selective
 67 detectors for GC × GC, there has been a noticeable amount of
 68 development for the aforementioned MS-technologies over the
 69 last decades mainly regarding mass accuracy and mass
 70 resolution^{21–23} as well as different ionization techniques,^{24–26}
 71 all of which have demonstrated their benefits. Having said this,
 72 restrictions concerning the analysis of isomeric, isobaric, small
 73 and very fragile compounds still remain. As GC × GC is quickly
 74 gaining importance in fields of complex sample analysis²⁷ there
 75 is an increasing interest in alternative detection systems for GC
 76 × GC.

77 A further class of interesting GC and GC × GC detectors are
 78 spectroscopic detectors, using light absorption or emission
 79 processes for fast and highly selective detection. Infrared (IR)
 80 spectroscopy²⁸ and atomic emission spectrometry²⁹ have been
 81 successfully applied in conjunction with GC or GC × GC.
 82 These spectroscopic methods provide very specific and
 83 complementary information to MS which includes the
 84 distinguishability between structural isomers or elemental
 85 compositions. A critical point in combination with GC × GC
 86 is the demanded high acquisition frequency. For spectroscopic
 87 detectors this criterion will be only sufficiently fulfilled if the
 88 spectra are collected simultaneously. This is technically realized
 89 by either a detection based on light separation (dispersion or
 90 diffraction and array detector) or Fourier transform (FT)
 91 analysis (e.g., FT-IR). Unfortunately the application of IR based
 92 systems is restricted due to insufficiently low sensitivity caused
 93 by small molecular absorption cross sections in the infrared
 94 range. For the same reason gas phase ultraviolet (UV)
 95 spectroscopy has rarely been applied as a GC detector^{30,31}
 96 and has also not been extensively established as a GC × GC
 97 detector. However, the molecular absorption cross section in
 98 the vacuum ultraviolet region (VUV) is generally by orders of
 99 magnitude larger than it is in the IR or UV. Therefore, the use
 100 of the VUV-absorption region for spectroscopic detection is
 101 very promising as it will result in orders of magnitude higher
 102 sensitivities than that of classical UV detection; although, the
 103 fingerprint selectivity in the gas phase UV spectroscopy is often

higher.^{32,33} The higher sensitivity in the VUV-range allows fast
 104 and sensitive spectroscopic detection and it is also possible to
 105 draw structural and isomer-selective information from the
 106 VUV-absorption spectra.³⁴ These alluring factors motivate the
 107 use of VUV-absorption techniques for complex matrixes. The
 108 first VUV-absorption detection systems applied for GC were
 109 limited to a narrow band of vacuum-UV radiation, or even only
 110 to single wavelengths, which resulted in no qualitative
 111 information.^{35,36} Consequently, a simultaneous VUV-absorption
 112 spectrometer was introduced by Lagesson et al.^{37,38} in
 113 1998 providing quantitative and qualitative analysis with good
 114 detection, classification, and identification limits in the
 115 wavelengths range between 168 and 330 nm.
 116

117 Recently, a matured simultaneous vacuum ultraviolet
 118 absorption spectroscopy system was introduced which provides
 119 full absorption spectra in the accessible wavelengths-region
 120 down to 125 nm within milliseconds.³⁹ In the aforementioned
 121 spectral range, all organic chemical compounds absorb VUV-
 122 radiation strongly resulting in very rich and selective
 123 spectrometric information. This VUV-detector is considered
 124 the first ultraviolet absorption based detector that complies
 125 with the requirements for GC × GC and operates with
 126 promising analytical performance characteristics to an MS
 127 regarding the speciation of compounds. In this work a VUV-
 128 absorption spectroscopy based detector was hyphenated to a
 129 GC × GC system in order to demonstrate and explore the gain
 130 in qualitative information due to the integration of VUV
 131 spectral information to GC × GC, which has not been reported
 132 in literature before.

133 ■ EXPERIMENTAL SECTION

134 **VUV Absorption Detector.** The working principle of the
 135 VUV-spectrometer VGA-100 (VUV Analytics, Inc., Austin, TX)
 136 has been described elsewhere.³⁹ Briefly, the eluent from the gas
 137 chromatographic column is directly fed into a 10 cm long
 138 absorption flow cell and the broad band light emission from a
 139 high power deuterium lamp is diffracted by means of a
 140 holographic grating after passing through the flow cell in the

141 same direction as the eluent. Wavelengths in the range of 125–
142 240 nm are focused onto a back-thinned charge-coupled device
143 (CCD)-array detector. For GC × GC setup A, a prototype, and
144 for GC × GC setup B, a further developed commercially
145 available detector, was applied. The system used for GC × GC
146 setup B had an advanced flow path with reduced void volume.

147 **GC × GC Setups.** The hyphenation between the GC × GC
148 and the VUV-detector were accomplished by means of directly
149 coupling to the second dimension capillary column (Figure
150 1A). Two different GC × GC setups were applied.

151 Setup A: For the first experiments comprising the one-
152 dimensional GC measurements as well as the two-dimensional
153 analysis of the diesel and syncrude, a VGA-100 detector (VUV
154 Analytics, Austin, TX) was directly coupled to an Agilent 6890
155 gas chromatograph from a LECO GC × GC-FID (LECO, St.
156 Joseph, MI, USA). The samples were directly injected at 250
157 °C with a split ratio of 1:50 using helium as carrier gas. The GC
158 oven was programmed with a constant column flow of 1.2 mL/
159 min starting at a temperature of 60 °C which was held for 2
160 min, ramped up to 320 °C and held for 10 min. The
161 temperature of the transfer line to the VUV-spectrometer was
162 set to 250 °C. Chromatographic separation in the first GC
163 dimension was carried out on a 60 m × 0.25 mm i.d. × 0.25 μm
164 BPX5 capillary column (SGE Analytical Science, Ringwood,
165 Australia). For GC × GC-VUV-analysis a 2 m × 0.25 mm i.d. ×
166 0.25 μm BPX50 capillary column (SGE Analytical Science,
167 Ringwood, Australia) was chosen for the second dimension and
168 directly connected to a 0.25 mm i.d. transfer capillary. The
169 makeup gas (pure nitrogen >5.0) was set to 0.4 psi to control
170 the residence time of the compounds within the flow cell of the
171 VGA-100. According to the given peak width an acquisition
172 frequency of 50 Hz was chosen for two-dimensional gas
173 chromatography and 5 Hz for one-dimensional application.
174 (Variable parameters are listed in Supporting Information table
175 S1).

176 Setup B: For quantitative measurements and comparison to
177 GC × GC-TOFMS, a further developed VGA-100 detector was
178 connected to an Agilent 7890A equipped with a ZOEX ZX1
179 modulator. A HTOF (TOFWerk, Thun, Switzerland) was
180 taken as reference. For the analysis the following column
181 combination was applied: 30 m × 0.25 mm × 1 μm 007-FFAP
182 column (Quadrex, Woodbridge, USA) + 3 m × 0.1 mm × 0.5
183 μm 007-1701 column and a makeup gas of pressure of 1.5 psi.

184 **Sample Material.** A common diesel fuel with up to 7% bio
185 diesel constituent (fatty acid methyl ester, FAME) and two
186 Fischer–Tropsch (FT) syncrudes (high and low temperature
187 iron catalyzed FT processes) were analyzed using GC and/or
188 GC × GC-VUV. The diesel fuel is a standard German B7 diesel
189 fuel from a petro station according to DIN EN 590.
190 Information about similar diesel fuel compositions based on
191 the GC × GC-TOFMS data have already been published.⁷ The
192 FT syncrudes were generated in a laboratory fixed bed FT-
193 bench reactor by means of an iron based polymeric catalyst
194 reaction at the University of Rostock. The FT reactor was
195 operated at 250 °C (low temperature FT sample) and at 350
196 °C (high temperature FT sample). Complementary GC × GC-
197 TOFMS were recorded as well.

198 **Data Handling.** The chromatographic data were recorded
199 as a one-dimensional data string composed of the subsequently
200 but simultaneous acquired VUV-absorption spectra. The data
201 acquisition of the VUV-system is designed for a maximum duty
202 cycle leading to nonuniformly spaced time vectors while
203 spectral data were stored uniformly from 125 to 240 nm with

0.05 nm increments. Time resolved predefined summed
wavelength domains (125–240 nm, 140–165 nm, and 170–
200 nm) and full spectral data were exported separately in an
ASCII format. For matrix operations, and two-dimensional
visualization, the data were interpolated to a 20 ms uniformly
spaced time vector and reshaped to build up a two- (summed
wavelength domains) or three- (spectral data) dimensional data
array. The size of the array was defined as following: first
dimension = number of modulation cycles (“retention time first
dimension”), second dimension = modulation time ×
acquisition frequency (“retention time second dimension”),
third dimension (if applicable) = spectral range with an
increment of 0.05 nm. Two dimensional plots as well as volume
plots were generated with MatLab (R 2013b).

RESULTS AND DISCUSSION

Chromatography and Peak Shape. Both generations of
the applied VGA-100 detector were designed for the hyphen-
ation with one-dimensional gas chromatography (1DGC) and
peak shape as well as peak width are influenced by the applied
make up gas flow. When a typical makeup gas pressure for
1DGC of 0.05 psi was utilized, a peak width of 2 s (fwhm) was
obtained. This, however, is too long for GC × GC applications
and therefore, the makeup gas pressure was increased stepwise
to 0.4 psi for setup A and 1.5 psi for setup B. For both setups
this resulted in a reduced peak width of approximately 300 ms
fwhm (Table 1) and an almost Gaussian peak shape. A further

Table 1. Comparison between GC × GC-TOFMS and GC × GC-VUV for Selected Compounds

		GC × GC- TOFMS	GC × GC-VUV
peak width (ms)	benzene	170	300
	<i>n</i> -hexane	100	300
limit of detection (ng)	benzene	0.1	16
	<i>n</i> -hexane	0.07	7

increase of the makeup gas pressure led to a substantial
decrease in peak height. The observed peak bordering
compared to GC × GC-TOFMS (Table 1) was referred on
the one hand to different flow conditions (vacuum outlet for
TOFMS and slightly elevated ambient pressure for VUV) and
on the other hand to the residence time within the flow cell (1
mm i.d. and 80 μL) of the VGA-100 prototype. Smaller inner
diameter⁴⁰ flow cells are currently under investigation but were
not available for the experiments. Table 1 also list the received
detection limits for the compounds. The sensitivity of the
system would gain from a smaller inner diameter of the flow
cell due to a higher absorbance and smaller makeup gas flows.
The special design of the applied VUV detector would also
recommend the use of a flow modulator since high flow rates
the second dimension are compatible with the detector.

Spectroscopy. The obtained VUV-absorption spectra
reflect mainly the interaction of electrons of the higher
occupied molecular orbitals of the gas phase molecules with
VUV-photons.¹⁹ Unlike scanning instrumentation, where
individual transitions are excited mainly independently, the
molecules are exposed to a continuous broadband VUV-
emission from a strong deuterium light source. The shorter-
wavelength photons also exceed the ionization- and dissociation
energies of most organic compounds, leading to the presence of
some ionized or photolyzed species in the measuring volume.⁴¹

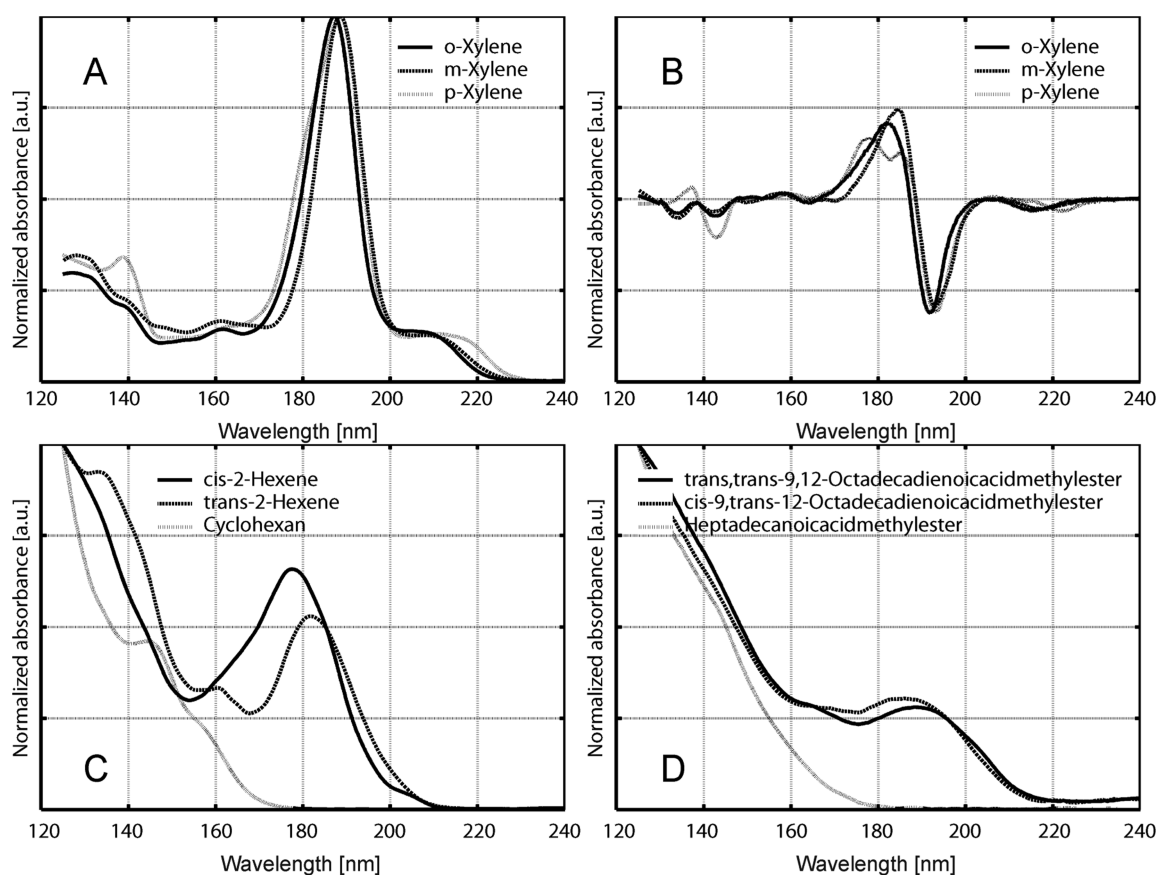


Figure 2. VUV spectra and first derivation of VUV spectra for different types of isomers. (A) VUV spectra of xylene position isomers. Spectra are dominated by $\pi^* \leftarrow \pi$ transition between 170 and 200 nm. Distinct features will allow a differentiation. (B) First derivative of VUV spectra of xylene. *o*- and *m*-Xylene show similar shapes. Derivative of *p*-xylene indicate a shoulder in the $\pi^* \leftarrow \pi$ region and a second local maximum in the $\sigma^* \leftarrow \sigma$ region. (C) Common separation problem in GC \times GC/MS: differentiation of compounds which have similar retention characteristics (GC \times GC) as well as similar 70 eV fragmentation pattern (MS). VUV spectroscopy allows an explicit differentiation of these compounds. (D) VUV spectra for selected higher boilers in middle distillates. Also larger isomeric compounds show distinct spectral features.

255 Also secondary chemical reactions such as chemical ionization
 256 by proton transfer may occur.⁴² Although, the relative
 257 concentration of photoradicals and ions is supposedly relatively
 258 low, the absorption of photochemical products might explain
 259 the observed differences in the appearance of VUV-spectra
 260 obtained with scanning or simultaneous VUV-spectrometers.
 261 The spectral acquisition range of the detector is restricted to
 262 125–240 nm due to the low end cutoff of the MgF₂ windows.
 263 The used early stage of the system did not correct for higher
 264 order reflection; therefore, the spectral range over 240 nm is
 265 not shown. In the accessible range, low lying $\sigma^* \leftarrow \sigma$, $\sigma^* \leftarrow n$,
 266 $\pi^* \leftarrow \pi$, and $\pi^* \leftarrow n$ transitions can be excited and are
 267 responsible for the VUV-light adsorption.

268 Figure 1B shows the VUV-spectrum of benzene acquired
 269 with the VUV-spectrometer as well as a reference spectrum
 270 from the literature.¹⁹ The intense and characteristic p-band as
 271 well as the β -band of the electronically allowed and the
 272 forbidden $\pi^* \leftarrow \pi$ singlet transitions qualitatively corresponds
 273 with the reference spectrum. The information content of MS as
 274 well VUV spectroscopy is mainly dependent on the spectral
 275 resolution of the system and nowadays state-of-the-art high-
 276 resolution and accurate mass time-of-flight technology allows
 277 the calculation of elemental composition and decomposition of
 278 the isotopic pattern. This could be thought as a fingerprint of
 279 the compound.²¹ The resolutions of both spectra shown in
 280 Figure 1B are not sufficient to make a distinct assignment of

vibronic transitions. In particular, the rotational and vibrational 281
 fine structure is not or only in a limited manner accessible. 282
 Therefore, filtering or scripting approaches may not address the 283
 selectivity of such very discrete transitions. Moreover, they rely 284
 on target selective discriminating characteristics of the shape of 285
 the absorption bands. Mathematically, distinct features like 286
 extrema, saddle points, or shoulders could be found by the first 287
 or higher derivative of the spectra (Figure 2). Nevertheless, the 288
 spectral information allows also differentiation of closely related 289
 structural isomers and the coincidence of very high attenuation 290
 coefficients with the emission maxima of common deuterium 291
 lamps lead to low achievable detection limits. 292

Investigation of Diesel Fuel with One-Dimensional 293
Gas Chromatography VUV Absorption Spectroscopy 294
and Concept for Spectroscopic Filtering. The investigated 295
 diesel matrix is a blend of petrochemical derived diesel with a 296
 defined mixture of fatty acid methyl esters (FAME, “bio diesel” 297
 constituent). Because of the refinery and upgrading process, the 298
 petroleum matrix is as mixture of saturated alkanes (linear, 299
 branched, and cyclic), aromatic hydrocarbons, and their 300
 condensation and alkylation products. Unsaturated aliphatic 301
 molecular structures as well as carboxylic structures are only 302
 introduced by the FAME mixture. Other organic compounds 303
 bearing heteroatoms, such as benzofurans or benzothiophenes 304
 are present only at low trace levels and are not considered. The 305
 $\sigma^* \leftarrow \sigma$ chromophoric contribution of the absorption spectra is 306

307 mainly caused by the C–C and C–H bonds. These transitions
 308 are only excited in the far VUV-range below 190 nm and could
 309 be detected very sensitively due to their very high ϵ .
 310 Consequently, common GC-UV systems working only up to
 311 the near VUV-range could not address compounds which
 312 exclusively exhibit $\sigma^* \leftarrow \sigma$ chromophores, even if they are
 313 predominant ingredients of the matrix (e.g., alkanes in
 314 petrochemical matrixes, examples shown in Figure 2). Since
 315 isolated double bonds do not occur in fully processed and
 316 standardized middle distillate diesel (without FAME), the $\pi^* \leftarrow \pi$
 317 contribution could be exclusively assigned to conjugated
 318 double bonds of aromatic structures. Therefore, the wave-
 319 lengths region of (170–200 nm) can be used to selectively
 320 detect (i.e., “filter out”) compounds with aromatic $\pi^* \leftarrow \pi$
 321 chromophores for the given matrix. In mass spectrometry,
 322 unique (mass) spectral features are already used for the
 323 assignment to substance classes and very complex algorithm
 324 can be applied to, e.g., 70 eV electron impact (EI)
 325 fragmentation spectra, which is known as scripting.^{43,44} Figure
 326 3 shows the adaption of this filter concept to GC-VUV-data.

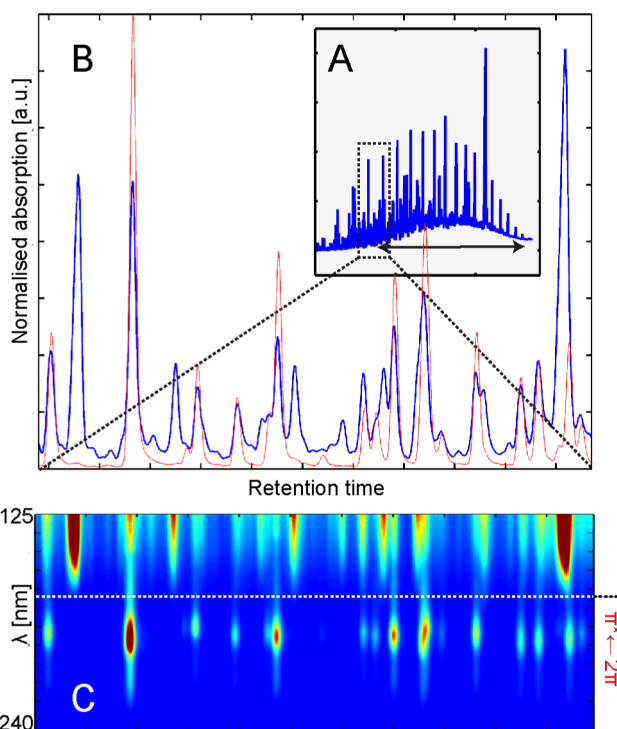


Figure 3. One-dimensional chromatographic separation of B7 Diesel fuel with VUV-detection. (A) Total absorption signal. Vertical arrow indicate chromatographically not sufficiently resolved region. (B) Enhancement of partial chromatographically resolved region. Blue, total absorption signal; red, summed absorption signal within spectral range of filter (170–200 nm) for selection of compounds with $\pi^* \leftarrow \pi$ chromophores. (C) Corresponding two-dimensional representation of part B.

327 However, while $\sigma^* \leftarrow \sigma$ transitions are not very class specific,
 328 the $\pi^* \leftarrow \pi$ transition is a unique feature for the presence of
 329 aromatic or unsaturated structures. For a defined matrix
 330 without alkenes like diesel, this absorption can be exclusively
 331 attributed to aromatic compounds. The first part of the 1DGC
 332 chromatogram (Figure 3) is dominated by a limited number of
 333 alkyl substituted benzenes,⁷ which could be visualized even
 334 within a very complex matrix of alkane isomers. Differentiation

of individual peaks is well possible and even deconvolution of
 peaks based on VUV-spectra has already been demonstrated for
 xylene isomers³⁹ and gasoline. However, gasoline has a simpler
 composition due to its relatively limited carbon number
 distribution and lower boiling point. Diesel fuel in contrast
 exhibits a much higher complexity and only the early eluting
 compounds can be sufficiently separated by 1DGC. For later
 eluting fractions, more selective chromatographic separation
 approaches are required. For such cases, the achieved peak
 widths and shapes allow the application of the detector for
 comprehensive two-dimensional gas chromatography.

Investigation of Diesel Fuel with Comprehensive Two-Dimensional Gas Chromatography VUV Absorption Spectroscopy. The VUV-spectral data could be assumed to be widely orthogonal to GC-separation whereas some mass spectrometric information is highly related to the retention times of the molecules. Especially the molecular mass, one of the most selective information in GC \times GC/MS, is highly related (nonorthogonal) to the elution order of the corresponding compound and becomes obvious for soft ionization techniques like photoionization.²⁴ Figure 4A shows the typical structured pattern of GC \times GC separation for middle distillates. Z-intensities reflect the summed VUV-absorption (125–240 nm) and could be compared to total ion current in mass spectrometry. Saturated and branched alkanes are the dominant peaks caused by both their high relative concentrations and also very high absorption cross sections or ϵ . While cyclic alkanes are clearly extracted from the bulk of linear and branched compounds, a coelution with alkenes could not be excluded based on GC \times GC separation.⁴⁵ The presence of reactive compounds like alkenes would affect the storage stability of the fuel in a negative manner. Also additional mass spectrometric information often fails to differentiate the compounds. However, VUV-spectral data clearly indicate the absence of $\pi^* \leftarrow \pi$ chromophores in the corresponding chromatographic elution region for alkenes (Figure 4B). The application of the 170–200 nm $\pi^* \leftarrow \pi$ filter also confirms the locations of the aromatic compounds. Because of their high absorption polyaromatic compounds are also evident despite the fact that their spectral maxima are outside the spectral range of the filter and only the tails of the absorption peaks contribute. According to the elution pattern of aromatic compounds for the given chromatographic system, the row of substituted benzenes are eluting first from the second dimension followed by condensed aromatic-cyclic compounds and polyaromatic hydrocarbons. Unlike aromatics, FAMEs are only partially discriminated by the filter. Fully saturated FAMEs have their main absorption almost exclusively below 170 nm while the $\pi^* \leftarrow \pi$ chromophores in unsaturated FAMEs will also absorb very strongly within the range of the filter. A comparison of the filtered and unfiltered chromatograms qualitatively indicates the high amount of not fully saturated FAMEs. While the C16 fraction is dominated by C16:0, the C18 fraction is dominated by C18:1 and higher unsaturated FAMEs.⁷ Therefore, C16 FAMEs are not shown in the filtered chromatogram while C18:1 and C18:2 are still dominating coeluting peaks due to their high concentrations.

Investigation of Fischer–Tropsch syncrude with Comprehensive Two-Dimensional Gas Chromatography VUV Absorption Spectroscopy. Fischer–Tropsch (FT) syncrude is an intermediate product in fuel production from fossil as well bigenic sources. At this stage it is not refined or upgraded like diesel. Because of a defined syngas composition

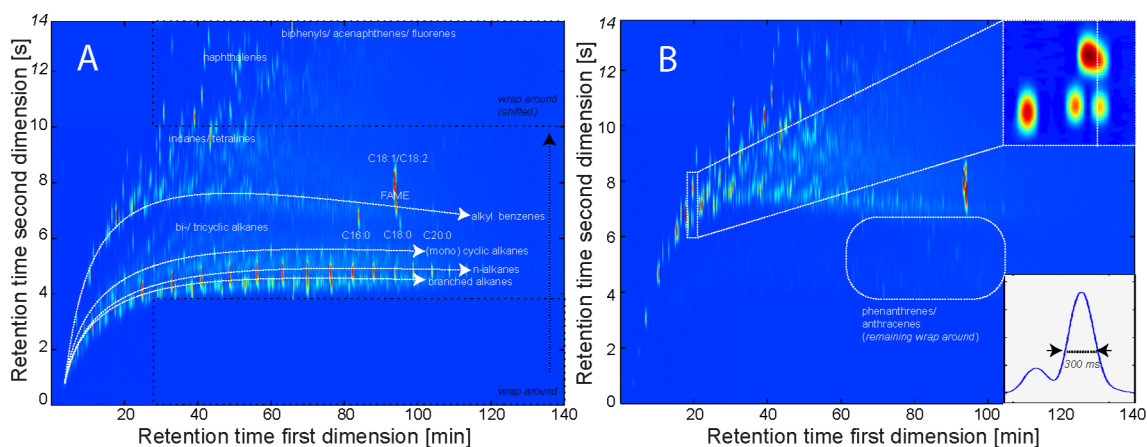


Figure 4. Application of spectral filters for different petrochemical matrices. (Highlighted regions are described in the [Results and Discussion](#), all chromatograms show some degree of wrap around.) (A) GC \times GC-VUV-chromatogram of B7 diesel fuel (total VUV-absorption 125–240 nm). (B) Application of 170–200 nm filter to (A) for the discrimination of $\pi^* \leftarrow \pi$ chromophores. Compounds with solely $\sigma^* \leftarrow \sigma$ chromophores will disappear.

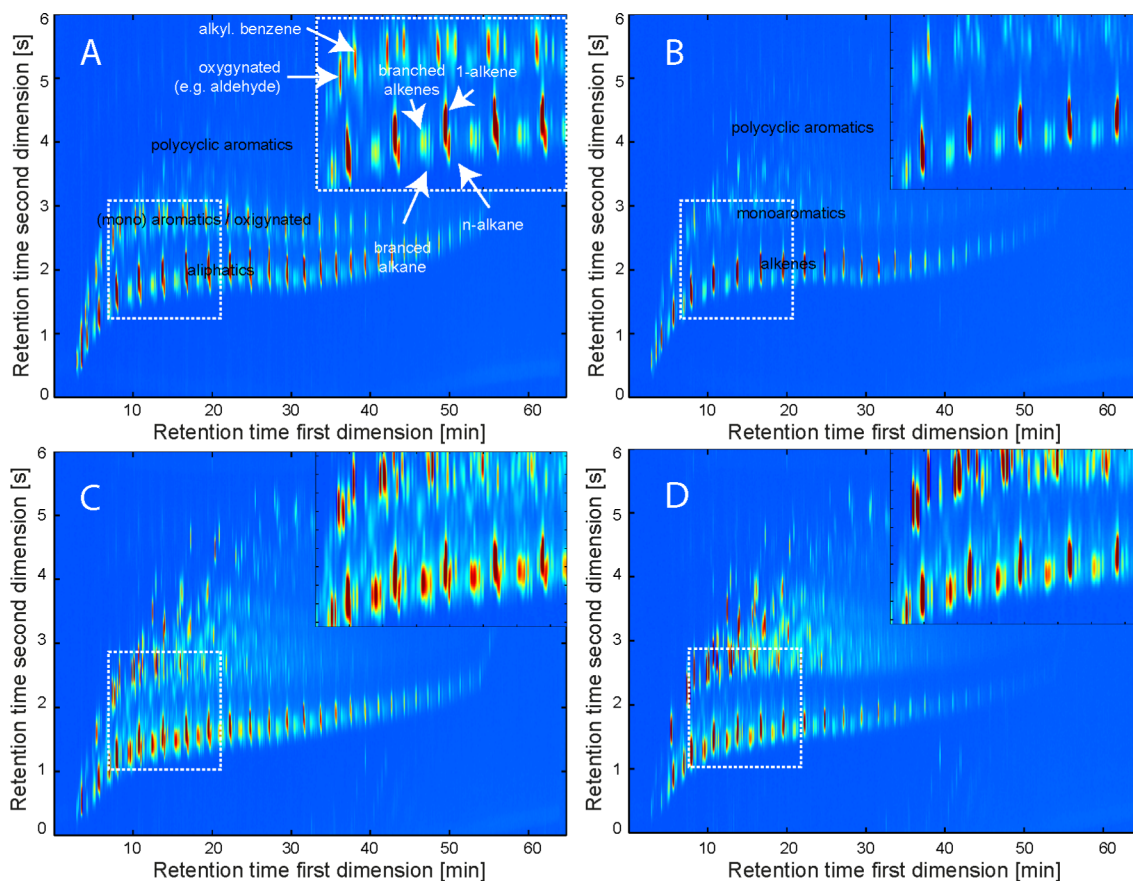


Figure 5. (A) GC \times GC-VUV-chromatogram of low temperature Fischer–Tropsch (LTFT) syncrude (total VUV-absorption 125–240 nm). (B) Application of 170–200 nm filter to for the discrimination of $\pi^* \leftarrow \pi$ chromophores. The filter also allows for some discrimination of oxygenated compounds. (C) GC \times GC-VUV-chromatogram of high temperature Fischer–Tropsch (HTFT) syncrude (total VUV-absorption 125–240 nm). (D) Application of 170–200 nm filter to for the discrimination of $\pi^* \leftarrow \pi$ chromophores. The filter also allows some discrimination for oxygenated compounds.

398 and pretreatment of the syngas, the compounds within
 399 syncrude will be composed almost exclusively by C, H, and
 400 O (like B7 diesel). Trace impurities like metals and gasification
 401 artifacts, e.g., pyrolysis liquids, are not considered. Main
 402 differences are the high abundance of unsaturated and
 403 oxygenated compounds. Alkenes are quantitatively dominating

($\gg 10\%$), followed by different species of oxygenated and
 404 aromatic compounds. The exact composition of the syncrude is
 405 also affected by the reactor parameters like temperature and the
 406 catalyst which is used. Typical parameters which are associated
 407 with a shift toward higher temperatures are an increase of the
 408 degree of unsaturation (aromatics and alkenes) associated with
 409 15

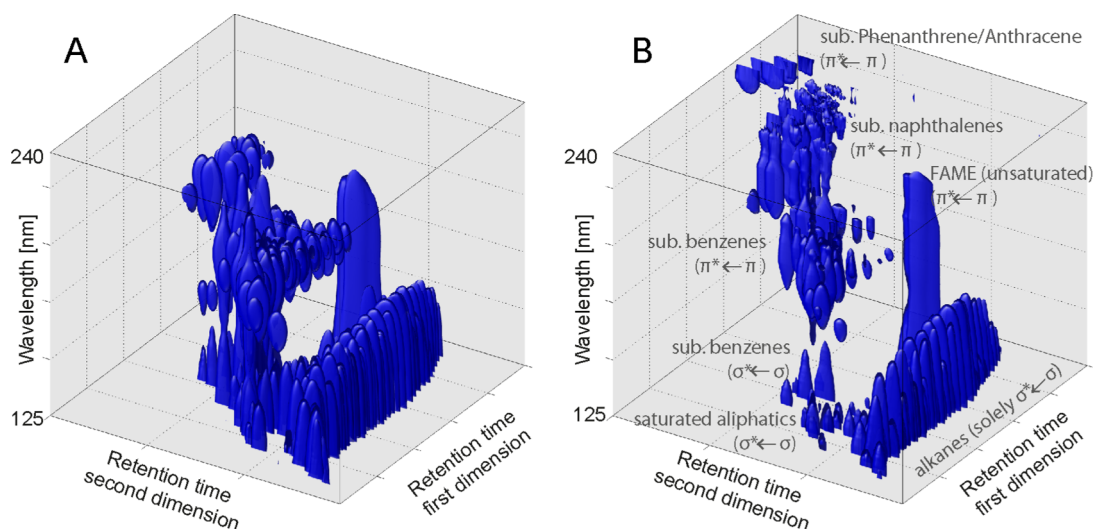


Figure 6. Three-dimensional illustration of B7 fuel analyzed with GC \times GC-VUV. (A) Raw VUV-spectra are arranged along the Z axis. Only the highest absorption regions are depicted. For details see the text. (B) Same matrix as (A) but each VUV-spectrum was normalized to 1. The normalization makes also compounds with lower concentrations visible (here the condensed ring aromatics).

410 a higher degree of branching. Figure 5 show two examples for a
 411 low and high temperature Fischer–Tropsch syncrude analyzed
 412 by GC \times GC-VUV. For these experiments, GC \times GC was
 413 operated under “screening” conditions, applying a fast heating
 414 rate of 5 K/min (Table S1). The total run time will decrease
 415 while the elution temperature of the compounds will increase
 416 compared to lower ramping rates. Therefore, retention times
 417 on the first and second dimension will be reduced with the
 418 drawback of a reduced separation power. Saturated and
 419 unsaturated compounds will overlap to a greater extent and
 420 for the given example, e.g., alkanes are only shifted slightly from
 421 the dominating alkenes. In addition also a well know separation
 422 problem for GC \times GC-TOFMS, namely, the separation of
 423 cyclic alkanes and alkenes⁴⁵ in petrochemical matrixes will
 424 aggravate but could be addressed by the application of VUV-
 425 spectroscopy. The already mentioned spectral filter 170–200
 426 nm clearly discriminates between unsaturated and saturated
 427 aliphatics even in cases of partial overlap. For the given
 428 example, the row of normal alkanes vanishes in the spectral
 429 filtered chromatograms. The HTFT syncrude also indicates a
 430 relatively higher constituent of branched alkenes. The spectra of
 431 oxygenated species are more complex. While they have usually
 432 very strong absorbance in the region below 170 nm, they could
 433 have also some absorption within the region of the applied
 434 spectral filter 170–200 nm. In particular, very small oxygenated
 435 compounds (<3 C atoms) show very distinct absorption
 436 spectra with isolated high absorption bands above 170 nm.
 437 Oxygenated with longer (linear) alkyl chains have only weak
 438 and broad bands above 170 nm. Therefore, a fading or
 439 complete disappearing of peaks in the region of benzenes could
 440 indicate the presence of oxygenated compounds. In the case of
 441 LTFT especially the linear oxygenated compounds are present
 442 and discriminated by the applied filter. The remaining peak in
 443 this region of the chromatogram could be identified as
 444 benzenes which are much more dominant in HTFT. The
 445 results presented are consistent with the expected composition
 446 of HTFT and LTFT syncrude and have been confirmed by GC
 447 \times GC-HRT (not shown).

448 **Visualization of GC \times GC-VUV Data for Data**
 449 **Interpretation.** The two-dimensional GC \times GC-retention
 450 time data can be also combined directly with the VUV-

spectroscopic data to produce a three-dimensional representa- 451
 452 tion. Figure 6 shows the three-dimensional visualizations of the 453
 454 B7 diesel fuel matrix GC \times GC-VUV-measurement (see Table 455
 456 S1 for different GC \times GC parameter). The *x*- and *y*-axes 457
 458 represent the two-dimensional GC \times GC retention time plane 459
 460 while the *z*-axis comprises the VUV-spectroscopic information. 461
 462 For Figure 6a, the spectroscopic raw signal was incorporated 463
 464 and the volume plot was performed with a cut off level of 0.2 465
 466 absorbance unit. For better visualization, the spectroscopic 467
 468 resolution was reduced to 1 nm during post processing. The 469
 470 size of the volumes is significantly influenced by the 471
 472 concentration of the individual compounds and their ϵ , 473
 474 hence, compounds in low abundance are suppressed due to 475
 476 the applied cut off level. Therefore, compounds in high 477
 478 concentration and/or those possessing strongly absorbing 479
 480 chromophores dominate the plot. The visual appearance of 481
 482 the different compounds shows some similarities to GC \times GC- 483
 484 SPITOFMS where the *z*-axis would reflect the mass 485
 486 spectrometric information.²⁴ 487
 488

489 Characteristic features of the VUV-spectra can also be 490
 491 visualized through normalization of the spectra. In Figure 6B, 492
 493 each spectra is normalized to 1. The normalization will 494
 495 emphasize the position of the absorption maxima within the 496
 497 spectral range, which is a basic target for filtering approaches. 498
 499 The analogue classifier approach for mass spectrometry is 500
 501 known as “domain knowledge based rules”.⁴⁶ Because of the 502
 503 selected column combination, saturated hydrocarbons elute at 504
 505 very early second dimension retention times and their spectra 506
 507 are dominated by high absorption tails tending toward the high 508
 509 energetic end of the spectral range of the detector. (The actual 510
 511 absorption maxima for the $\sigma^* \leftarrow \sigma$ transition of alkanes is 512
 513 outside the spectral range of the detector, around 80 nm). On a 514
 515 first glance, the bands of the alkanes look very similar and the 516
 517 cross section of the alkanes in the volatility range of the diesel 518
 519 matrix is increasing only moderately. More specific information 520
 521 is gained from a closer inspection of the shape of the tail, which 522
 523 will allow some within-group discrimination for, e.g., isomeric 524
 525 structures (Figure 2). For the given defined matrix a 526
 527 combination of the regional information from GC \times GC 528
 529 with this spectral characteristics will give a sufficient classifier 530
 531 for alkanes but it cannot be used as a bijective global classifier 532

492 for this compound class, since virtually all organic compounds
493 will have $\sigma^* \leftarrow \sigma$ transitions. More class selective are the
494 regions for the $\pi^* \leftarrow \pi$ transitions. With a higher number of
495 condensed aromatic systems, the maxima are shifted substan-
496 tially to the red while within-group variations are only moderate
497 and, e.g., the already mentioned filter of 170–200 nm will
498 discriminate pure saturated aliphatic compounds from aromatic
499 structures in a defined GC \times GC region for the given matrix.

500 ■ CONCLUSION

501 The introduced fast VUV-absorption detector shows great
502 potential to become a complementary selective and universal
503 detector for GC \times GC next to mass spectrometry. Extension of
504 the spectral range toward the higher energetic VUV-region
505 substantially enhances the sensitivity and selectivity of the
506 measured spectral information. In combination with the
507 regional information on GC \times GC, overall group specific
508 spectral information allows a discrimination of compound
509 classes by filtering or scripting. At the same time small
510 differences in the absorption characteristics of homologous and
511 isobaric compounds will also facilitate a discrimination of these
512 compounds and will give complementary information to mass
513 spectrometric information. The application of these features to
514 different petrochemical matrixes could also demonstrate the
515 adaptability to important applications in the field of very
516 complex matrixes.

517 ■ ASSOCIATED CONTENT

518 ● Supporting Information

519 The Supporting Information is available free of charge on the
520 ACS Publications website at DOI: 10.1021/acs.anal-
521 chem.5b02472.

522 Table S1, GC- and VUV-parameters for shown data
523 (PDF)

524 ■ AUTHOR INFORMATION

525 Corresponding Author

526 *E-mail: thomas.groeger@helmholtz-muenchen.de.

527 Author Contributions

528 [†]T.G. and B.G. contributed equally.

529 Notes

530 The authors declare no competing financial interest.

531 ■ ACKNOWLEDGMENTS

532 Financial support by Sasol Group Services (Pty) Limited is
533 gratefully acknowledged.

534 ■ REFERENCES

- 535 (1) Giddings, J. C. *Anal. Chem.* **1984**, *56*, 1258A–1270A.
536 (2) Dorman, F. L.; Whiting, J. J.; Cochran, J. W.; Gardea-Torresdey,
537 J. *Anal. Chem.* **2010**, *82*, 4775–4785.
538 (3) Liu, Z.; Phillips, J. B. *J. Chromatogr. Sci.* **1991**, *29*, 227–231.
539 (4) von Muhlen, C.; Khummueng, W.; Zini, C. A.; Caramao, E. B.;
540 Marriott, P. J. *J. Sep. Sci.* **2006**, *29*, 1909–1921.
541 (5) Adahchour, M.; Beens, J.; Vreuls, R. J. J.; Brinkman, U. A. T.
542 *TrAC, Trends Anal. Chem.* **2006**, *25*, 726–741.
543 (6) Kehimkar, B.; Parsons, B.; Hoggard, J.; Billingsley, M.; Bruno, T.;
544 Synovec, R. *Anal. Bioanal. Chem.* **2015**, *407*, 321–330.
545 (7) Jennerwein, M. K.; Eschner, M.; Gröger, T.; Wilharm, T.;
546 Zimmermann, R. *Energy Fuels* **2014**, *28*, 5670–5681.
547 (8) Welthagen, W.; Schnelle-Kreis, J.; Zimmermann, R. N. *J. Aerosol*
548 *Sci.* **2004**, *35*, 17–28.

- (9) Kallio, M.; Hyotylainen, T.; Lehtonen, M.; Jussila, M.; Hartonen, 549
K.; Shimmo, M.; Riekkola, M. L. *J. Chromatogr. A* **2003**, *1019*, 251– 550
260. 551
(10) Goldstein, A. H.; Worton, D. R.; Williams, B. J.; Hering, S. V.; 552
Kreisberg, N. M.; Panić, O.; Górecki, T. *J. Chromatogr. A* **2008**, *1186*, 553
340–347. 554
(11) Brasseur, C.; Dekeirsschieter, J.; Schotsmans, E. M. J.; de 555
Koning, S.; Wilson, A. S.; Haubrugge, E.; Focant, J.-F. *J. Chromatogr. A* 556
2012, *1255*, 163–170. 557
(12) Schäffer, M.; Gröger, T.; Pütz, M.; Dieckmann, S.; 558
Zimmermann, R. *J. Forensic Sci.* **2012**, *57*, 1181–1189. 559
(13) de Vos, J.; Dixon, R.; Vermeulen, G.; Gorst-Allman, P.; 560
Cochran, J.; Rohwer, E.; Focant, J.-F. *Chemosphere* **2011**, *82*, 1230– 561
1239. 562
(14) Ly-Verdu, S.; Groeger, T. M.; Arteaga-Salas, J. M.; Brandmaier, 563
S.; Kahle, M.; Neschen, S.; de Angelis, M. H.; Zimmermann, R. *Anal.* 564
Bioanal. Chem. **2015**, *407*, 343–354. 565
(15) Shellie, R. A. *Aust. J. Chem.* **2005**, *58*, 619–619. 566
(16) Almstetter, M.; Oefner, P.; Dettmer, K. *Anal. Bioanal. Chem.* 567
2012, *402*, 1993–2013. 568
(17) Bean, H. D.; Hill, J. E.; Dimandja, J.-M. D. *J. Chromatogr. A* 569
2015, *1394*, 111–117. 570
(18) Blase, R. C.; Llera, K.; Luspay-Kuti, A.; Libardoni, M. *Sep. Sci.* 571
Technol. **2014**, *49*, 847–853. 572
(19) Engelke, F. *Aufbau der Moleküle*; Teubner: Stuttgart, Germany, 573
1985. 574
(20) Mondello, L.; Casilli, A.; Tranchida, P. Q.; Dugo, G.; Dugo, P. 575
N. J. Chromatogr. A **2005**, *1067*, 235–243. 576
(21) Ubukata, M.; Jobst, K. J.; Reiner, E. J.; Reichenbach, S. E.; Tao, 577
Q.; Hang, J.; Wu, Z.; Dane, A. J.; Cody, R. B. *J. Chromatogr. A* **2015**, 578
1395, 152–159. 579
(22) Franchina, F. A.; Machado, M. E.; Tranchida, P. Q.; Zini, C. A.; 580
Caramão, E. B.; Mondello, L. *J. Chromatogr. A* **2015**, *1387*, 86–94. 581
(23) Tranchida, P. Q.; Franchina, F. A.; Zoccali, M.; Panto, S.; 582
Sciarrone, D.; Dugo, P.; Mondello, L. *J. Chromatogr. A* **2013**, *1278*, 583
153–159. 584
(24) Eschner, M.; Welthagen, W.; Gröger, T.; Gonin, M.; Fuhrer, K.; 585
Zimmermann, R. *Anal. Bioanal. Chem.* **2010**, *398*, 1435–1445. 586
(25) Hejazi, L.; Ebrahimi, D.; Guilhaus, M.; Hibbert, D. B. *Anal.* 587
Chem. **2009**, *81*, 1450–1458. 588
(26) Wachsmuth, C. J.; Almstetter, M. F.; Waldhier, M. C.; Gruber, 589
M. A.; Nürnberger, N.; Oefner, P. J.; Dettmer, K. *Anal. Chem.* **2011**, 590
83, 7514–7522. 591
(27) Donato, P.; Cacciola, F.; Tranchida, P. Q.; Dugo, P.; Mondello, 592
L. *Mass Spectrom. Rev.* **2012**, *31*, 523–559. 593
(28) Grainger, J.; Li, Z.; Walcott, C.; Smith, C. J.; Patterson, D. G.; 594
King, B.; Gillyard, C. *Polycyclic Aromat. Compd.* **2002**, *22*, 489–500. 595
(29) van Stee, L. L. P.; Beens, J.; Vreuls, R. J. J.; Brinkman, U. A. T. *J.* 596
Chromatogr. A **2003**, *1019*, 89–99. 597
(30) Sanz-Vicente, I.; Cabredo, S.; Galban, J. *Chromatographia* **1998**, 598
48, 535–541. 599
(31) Cedrón-Fernández, T.; Sáenz-Barrio, C.; Cabredo-Pinillos, S.; 600
Sanz-Vicente, I. *Talanta* **2002**, *57*, 555–563. 601
(32) Ginter, M. L.; Yoshino, K. In *Vacuum Ultraviolet Spectroscopy*, 602
Samson, J. A., Ederer, D. L., Eds.; Academic Press: San Diego, CA, 603
2000; pp 263–277. 604
(33) Pratt, D. W. *Annu. Rev. Phys. Chem.* **1998**, *49*, 481–530. 605
(34) Fan, H.; Smuts, J.; Walsh, P.; Harrison, D.; Schug, K. A. *J.* 606
Chromatogr. A **2015**, *1389*, 120–127. 607
(35) Middleditch, B. S.; Sung, N.-J.; Zlatkis, A.; Settembre, G. 608
Chromatographia **1987**, *23*, 273–278. 609
(36) Driscoll, J. N.; Duffy, M.; Pappas, S. J. *Chromatogr. A* **1988**, *441*, 610
63–71. 611
(37) Lagesson-Andrasko, L.; Lagesson, V.; Andrasko, J. *Anal. Chem.* 612
1998, *70*, 819–826. 613
(38) Lagesson, V.; Lagesson-Andrasko, L.; Andrasko, J.; Baco, F. J. 614
Chromatogr. A **2000**, *867*, 187–206. 615

- 616 (39) Schug, K. A.; Sawicki, I.; Carlton, D. D.; Fan, H.; McNair, H.
617 M.; Nimmo, J. P.; Kroll, P.; Smuts, J.; Walsh, P.; Harrison, D. *Anal.*
618 *Chem.* **2014**, *86*, 8329–8335.
- 619 (40) Koek, M. M.; Muilwijk, B.; van Stee, L. L. P.; Hankemeier, T. J.
620 *Chromatogr. A* **2008**, *1186*, 420–429.
- 621 (41) Hanley, L.; Zimmermann, R. *Anal. Chem.* **2009**, *81*, 4174–4182.
- 622 (42) Li, D.-X.; Gan, L.; Bronja, A.; Schmitz, O. J. *Anal. Chim. Acta*
623 **2015**, *891*, 43–61.
- 624 (43) Weggler, B. A.; Groeger, T.; Zimmermann, R. J. *Chromatogr. A*
625 **2014**, *1364*, 241–248.
- 626 (44) Welthagen, W.; Schnelle-Kreis, J.; Zimmermann, R. N. J.
627 *Chromatogr. A* **2003**, *1019*, 233–249.
- 628 (45) van der Westhuizen, R.; Potgieter, H.; Prinsloo, N.; de Villiers,
629 A.; Sandra, P. J. *Chromatogr. A* **2011**, *1218*, 3173–3179.
- 630 (46) Vogt, L.; Groger, T.; Zimmermann, R. J. *Chromatogr. A* **2007**,
631 *1150*, 2–12.